Neurotoxicity Research (2019) 36:306–322
https://doi.org/10.1007/s12640-019-00054-6

CLINICAL RESEARCH REPORT

Breakdown of the Paracellular Tight and Adherens Junctions in the Gut and Blood Brain Barrier and Damage to the Vascular Barrier in Patients with Deficit Schizophrenia

Michael Maes[1,2,3] · Sunee Sirivichayakul[4] · Buranee Kanchanatawan[1] · Aristo Vodjani[5,6,7]

Received: 20 February 2019 / Revised: 29 March 2019 / Accepted: 23 April 2019 / Published online: 10 May 2019
© Springer Science+Business Media, LLC, part of Springer Nature 2019

Abstract

Deficit schizophrenia is characterized by leaky intestinal tight and adherens junctions and bacterial translocation. Here we examine whether (deficit) schizophrenia is accompanied by leaky paracellular, transcellular, and vascular barriers in the gut and blood-brain barriers. We measured IgA responses to occludin, claudin-5, E-cadherin, and β-catenin (paracellular pathway, PARA); talin, actin, vinculin, and epithelial intermediate filament (transcellular pathway, TRANS); and plasmalemma vesicle-associated protein (PLVAP, vascular pathway) in 78 schizophrenia patients and 40 controls. IgA responses to claudin-5, E-cadherin, and β-catenin, the sum of the four PARA proteins, and the ratio PARA/TRANS were significantly higher in deficit schizophrenia patients than in nondeficit schizophrenia patients and controls. A large part of the variance in PHEMN (psychosis, hostility, excitation, mannerism, and negative) symptoms, psychomotor retardation, formal thought disorders, verbal fluency, word list memory, word list recall, and executive functions was explained by the PARA/TRANS ratio coupled with plasma IgA responses to Gram-negative bacteria, IgM to malondialdehyde, CCL-11 (eotaxin), IgA levels of the ratio of noxious to more protective tryptophan catabolites (NOX/PRO TRYCATs), and a plasma immune activation index. Moreover, IgA levels to Gram-negative bacteria were significantly associated with IgA to E-cadherin, β-catenin, and PLVAP, while IgA levels to claudin-5 were significantly predicted by IgA to E-cadherin, NOX/PRO TRYCAT ratio, Gram-negative bacteria, and CCL11. The phenomenology of the deficit syndrome is to a large extent explained by the cumulative effects of lowered natural IgM, breakdown of the paracellular and vascular pathways, increased bacterial translocation, peripheral immune-inflammatory responses, and indices of BBB breakdown.

Introduction

Recently, we reported that deficit schizophrenia, PHEMN symptoms (indicating psychosis, hostility, excitation, mannerism and negative) and impairments in semantic and episodic memory are significantly associated with an upregulated intestinal paracellular pathway with breakdown of the tight (TJ) and adherens (AJ) junctions and increased bacterial translocation (Maes et al. 2018a, 2019). These conclusions were derived from findings that deficit schizophrenia and its phenomenological characteristics are accompanied by increased immunoglobulin (Ig)M responses to occludin and E-cadherin, which are both core transmembrane components of the TJs and AJs in the gut, and increased IgA/IgM responses to LPS of Gram-negative gut-commensal bacteria (Maes et al. 2018a, 2019). Occludin contributes to the stability and integrity of the TJs thereby regulating the permeability of the transcellular pathway (Yu et al. 2005; Suzuki et al. 2009; Elias et al. 2009; Furuse et al. 1993; Balda and Matter 2000; Cummins

✉ Michael Maes
dr.michaelmaes@hotmail.com; https://scholar.google.co.th/citations?user=1wzMZ7UAAAAJ&hl=th&oi=ao

1 Department of Psychiatry, Faculty of Medicine, Chulalongkorn University, Bangkok, Thailand

2 Department of Psychiatry, Medical University of Plovdiv, Plovdiv, Bulgaria

3 IMPACT Strategic Research Center, Barwon Health, Deakin University, Geelong, VIC, Australia

4 Faculty of Medicine, Chulalongkorn University, Bangkok, Thailand

5 Immunosciences Lab., Inc, Los Angeles, CA, USA

6 Cyrex Labs, LLC, Phoenix, AZ, USA

7 Department of Preventive Medicine, Loma Linda University, Loma Linda, CA, USA

Table 1 Classifications of the different paracellular, transcellular, and vascular proteins and their indices used in the current study

	Classification	GUT barrier	BBB	More specific to vascular barriers
Antigens (IgA)				
Occludin	Tight junctions	Yes	Yes	–
Claudin-5	Tight junctions	–	Yes	–
E-cadherin	Adherens junctions	Yes	–	–
β-Catenin	Adherens junctions	Yes	Yes	Yes
Plasmalemma vesicle-associated protein (PLVAP)	Endothelial–vascular	Yes	Yes	Yes
Talin	Cytoskeletal	Yes	Yes	
Actin	Cytoskeletal	Yes	Yes	
Vinculin	Cytoskeletal	Yes	Yes	–
Epithelial intermediate filament (EIF)	Cytoskeletal	Yes	Yes	–
Z unit weighted composite scores		–	–	
Occludin + claudin-5 + E-cadherin + β-catenin	Paracellular (PARA)	GUT + BBB		
Talin + actin + vinculin + EIF	Transcellular (TRANS)	GUT + BBB		
β-Catenin + PLVAP	Vascular route (VASC)	GUT + BBB		Yes
Claudin-5 + occludin + β-catenin	BBB		Yes	
E-cadherin + occludin + β-catenin	Gut	Yes		
PARA/TRANS	Paracellular versus transcellular	Yes	Yes	
PARA + VASC/TRANS	Paracellular + vascular versus transcellular	Yes	Yes	Yes

2012). E-cadherin (epithelial cadherin) is a key component of intestinal adherens junctions, which provide stability and cell–cell adhesion among epithelial cells of the paracellular pathway, modulate intracellular signaling, and regulate turnover of the actin cytoskeleton through binding with β-catenin (van Roy and Berx 2008; Gomez et al. 2015; Brüser and Bogdan 2017; Hartsock and Nelson 2008). Table 1 shows the characteristics of the different barriers and their junctions and key molecules. Interestingly, in our study (Maes et al. 2019), only very modest changes in IgM responses to cytoskeletal proteins, including talin, actin, and vinculin, were detected in schizophrenia, while the ratio of IgM responses against paracellular versus transcellular proteins was significantly increased in deficit schizophrenia as compared with nondeficit schizophrenia and controls. Actin microfilaments, a major component of the cytoskeleton, maintain the shape and structure of the cell and regulate transcription (Dominguez and Holmes 2011). Talin, another cytoskeletal protein, plays a key role in the attachment of microfilaments to cell membranes and, together with vinculin, links integrin adhesion molecules to the actin cytoskeleton (Burridge and Connell 1983). Vinculin anchors actin filaments to the membrane and promotes cell–matrix and cell–cell junctions thereby controlling cell shape (Goldmann 2002). All in all, these results indicate that, in deficit schizophrenia, increased translocation of Gram-negative bacteria is driven by an increased permeability of the intestinal paracellular pathway.

Aberrations in the paracellular pathway may be caused by trigger factors that are relevant to (deficit) schizophrenia, including immune activation, gut dysbiosis, gliadin hypersensitivity, and increased zonulin production (Maes et al. 2019). (a) Pro-inflammatory cytokines such as interleukin (IL)-6, interferon (IFN)-γ, and tumor necrosis factor (TNF)-α, which are all increased in schizophrenia (Roomruangwong et al. 2018b), may disassemble TJs and AJs and, consequently, upregulate the paracellular pathway (Al-Sadi et al. 2009, 2014; Utech et al. 2010; Bruewer et al. 2006). (b) Gut dysbiosis and gluten–gliadin sensitivity are observed in some patients with schizophrenia (Dohan and Grasberger 1973; Ergün et al. 2018; Rowland et al. 2017; Nguyen et al. 2018). (c) Schizophrenia is also accompanied by increased IgM responses to zonulin and a higher frequency of the haptoglobin (Hp)-2 phenotype (zonulin is pre-Hp-2) suggesting that increased levels of zonulin may have displaced proteins of the zona occludens with consequent upregulation of the paracellular pathway (Fasano 2012a, b). A leaky or (upregulated) paracellular pathway is the doorway to increased bacterial translocation, activated immune-inflammatory pathways, and autoimmunity explaining that this phenomenon is involved in immune and autoimmune disorders, including diabetes type I, celiac disease, inflammatory bowel disease, and schizophrenia (Fasano 2012a, b; Edelblum and Turner 2009; Maes et al. 2019).

Importantly, we reported that the upregulated paracellular leak pathway and increased bacterial translocation coupled with other biomarkers of schizophrenia significantly predicted

PHEMN (psychosis, hostility, excitation, mannerism and negative) symptoms, psychomotor retardation, formal thought disorders, and neurocognitive impairments, including semantic and episodic memory (Maes et al. 2019). Those biomarkers include lowered natural IgM to malondialdehyde (MDA), increased levels of CCL-11 or eotaxin, an endogenous cognition deteriorating chemokine (ECDC), increased IgA responses to neurotoxic and excitotoxic tryptophan catabolites (TRYCATs) versus more protective TRYCATs (NOX/PRO ratio), and an index of immune activation based on assays of IL-10, soluble IL-1 receptor antagonist (sIL-1RA), and macrophage inflammatory protein (MIP)-1 (Maes et al. 2019). Based on those results, we suggested that breakdown of TJs and AJs and the consequent translocation of Gram-negative bacteria may have induced the abovementioned neuroimmune pathways which all together may cause neuroprogression, namely dysfunctions in synaptic sampling, synaptic plasticity, synaptogenesis, neurogenesis, neuroprotection, etc. (Maes et al. 2019).

The assays of IgA responses to paracellular versus transcellular proteins should, in theory, provide a better index than IgM values because deficit schizophrenia is characterized by a deficit in natural IgM (Maes et al. 2018b), as indicated by lowered IgM responses to oxidatively specific epitopes (OSEs). Deficits in natural IgM, including MDA and azelaic acid and phospholipid structures, may hamper the interpretation of induced IgM responses to barrier proteins (Maes et al. 2019). Nevertheless, there are no data in schizophrenia whether IgA responses to paracellular (including occludin, E-cadherin, β-catenin, and claudin-5) and transcellular (including talin, actin, vinculin, and epithelial intermediate filament (EIF)) proteins are involved in the pathophysiology of (deficit) schizophrenia. β-Catenin plays a key role in cell–cell adhesion and stabilizing cell–cell contacts, while the β-catenin/E-cadherin complex regulates the integrity of the AJs (Tian et al. 2011; Nelson and Nusse 2004; Van den Bossche et al. 2012). EIF, which is together with actin one of the major cytoskeletal components of epithelial cells, mediates barrier functions in epithelial cells and protects together with other cytoskeletal proteins against microbial invasions (Geisler and Leube 2016).

Interestingly, there is a large functional overlap between the blood brain barrier (BBB) and gut epithelial cell barrier as they are both regulated by TJs and AJs, while occludin and claudin are key proteins of the paracellular TJs of the gut barrier and BBB (Vojdani and Vojdani 2019). Nevertheless, as explained above, E-cadherin is an AJ protein that is more specific to the gut barrier, whereas claudin-5 is more expressed in the TJs of the BBB (Rüffer and Gerke 2004; Ma et al. 2017, 2019) and enhances TJ functions in the BBB thereby regulating BBB permeability (Ma et al. 2017). Therefore, the assay of IgA levels to E-cadherin and claudin-5 may help to differentiate between paracellular aberrations in the BBB and gut.

Finally, there are no data on the function of the vascular barrier (Spadoni et al. 2016; Bouziat and Jabri 2015) in (deficit) schizophrenia. Not only the gut epithelial barrier but also the gut–vascular barrier protects against translocation of Gram-negative bacteria from the gut lumen into the blood, while β-catenin signaling in endothelial cells regulates the vascular barrier (Spadoni et al. 2016; Bouziat and Jabri 2015). Plasmalemma vesicle-associated protein (PLVAP) is another key component of the vascular endothelium that regulates vascular permeability and homeostasis and plays a role in leukocyte migration at inflammatory sites (Guo et al. 2016; Elgueta et al. 2016).

Hence, the current study was carried out to examine whether (deficit) schizophrenia is accompanied by leaky paracellular tight and adherens junctions and transcellular and vascular barriers by measuring IgA responses to occludin, claudin-5, E-cadherin, and β-catenin (paracellular barrier); talin, actin, vinculin, and EIF (transcellular barrier); and PLVAP and β-catenin (vascular barrier). The a priori hypothesis is that deficit schizophrenia is characterized by increased IgA responses to paracellular and vascular proteins, whereas there are no changes in IgA responses to transcellular proteins.

Subjects and Methods

Participants

In this study, we recruited 40 healthy controls and 79 patients with schizophrenia who were all recruited from the same catchment area, i.e., Bangkok, Thailand. All schizophrenia patients attended the Department of Psychiatry, King Chulalongkorn Memorial Hospital, Bangkok, Thailand. They all complied with the DSM-IV-TR diagnostic criteria for schizophrenia and were in a stabilized phase of illness. Moreover, patients with schizophrenia were allocated to two clinical subgroups, namely patients with and without deficit schizophrenia (Kirkpatrick et al. 1989). Normal controls were recruited by word of mouth and were excluded when they showed lifetime or current axis-1 DSM-IV-TR diagnoses and/or a positive family history of schizophrenia. We excluded schizophrenia patients with current lifetime diagnoses of other axis-1 DSM-IV-TR disorders including schizoaffective disorder, bipolar disorder, substance use disorders, major depression, and psycho-organic disorders. Furthermore, we excluded schizophrenia patients who suffered from acute psychotic episodes the year prior to the study. Other exclusion criteria for controls and patients were comorbidities with neurodegenerative/neuroinflammatory (including stroke, multiple sclerosis, and Parkinson's disease) and medical disorders (including COPD, inflammatory bowel disease, rheumatoid arthritis, lupus erythematosus, psoriasis, and diabetes types 1 and 2) and pregnant females. We also excluded patients and

controls when they ever had used immunomodulatory medications including glucocorticoids and when they used supplements with antioxidants or ω3-polyunsaturated fatty acids the months prior to the study.

All patients and controls as well as the guardians, parents, or close family members gave written informed consent prior to participation in our study. The study was conducted according to International and Thai ethics and privacy laws. Approval for the study (298/57) was obtained from the Institutional Review Board of the Faculty of Medicine, Chulalongkorn University, Bangkok, Thailand, which is in compliance with the International Guidelines for Human Research protection as required by the Declaration of Helsinki, The Belmont Report, CIOMS Guideline, and International Conference on Harmonization in Good Clinical Practice.

Measurements

Clinical Assessments

The diagnosis of schizophrenia was made by a senior psychiatrist specialized in schizophrenia employing the DSM-IV-TR diagnostic criteria and the Mini-International Neuropsychiatric Interview (MINI) in a validated Thai translation (Kittirathanapaiboon and Khamwongpin 2005). The same psychiatrist also made the diagnoses of primary deficit versus nondeficit schizophrenia using the Schedule for the Deficit Syndrome (Kirkpatrick et al. 1989). On the same day, the same psychiatrist completed sociodemographic and clinical data in patients and controls using a semistructured interview and assessed rating scales, namely the Scale for the Assessment of Negative Symptoms (SANS) (Andreasen 1989), the Brief Psychiatric Rating Scale (BPRS) (Overall and Gorham 1962), the Positive and Negative Syndrome Scale (PANNS) (Kay et al. 1987), the Fibromyalgia and Chronic Fatigue Syndrome Rating scale (FF) (Zachrisson et al. 2002), and the Hamilton Depression (HAM-D) and Anxiety (HAM-A) Rating Scales (Hamilton 1959, 1960).

In this study, we used the total scores on the SDS, SANS, and PANSS to score negative and positive symptoms. Furthermore, as explained previously, we computed *z* unit weighted composite scores based on the items of these different rating scales to assess specific symptom domains (Maes et al. 2018a, b; Sirivichayakul et al. 2018, 2019; Kanchanatawan et al. 2018b). Table 2 shows those symptom domains and their computation. On the same day as the clinical and diagnostic training, a master in mental health assessed the neuropsychological battery of the Consortium to Establish a Registry for Alzheimer's disease (CERAD-PN) (CERAD 1986) in controls and schizophrenia patients. We measured the verbal fluency test (VFT) to test fluency and semantic memory, the word list memory (WLM) to probe learning ability and verbal episodic memory, and word list recall, true recall (true recall) to probe verbal episodic memory recall. On the same day, we also assessed three executive tests of the CANTAB (CANTAB 2018), namely One Touch Stockings of Cambridge Probability Solved on First Choice (OTS_PSOFC), to probe spatial planning, and spatial working memory (SWM), namely

Table 2 Indices of the different symptom domains and biomarker composite scores used in the current study

Symptom domains and biomarker scores	*Z* unit weighted composite scores
Psychosis	Sum of *z* score of item 1 on the positive subscale of the PANSS (zPANNSP1, delusion) + zPANSSP3 (hallucinations) + zPANNSP6 (suspiciousness) + *z* score of item 11 of the BPRS (zBPRS11: suspiciousness) + zBPRS12 (hallucinatory behavior) + zBPRS15 (unusual thought content)
Hostility	Sum of zPANSSP7 (hostility) + *z* score of item 14 on the general psychopathology scale of the PANSS (zPANSSG14: poor impulse control) + zBPRS10 (hostility) + zBPRS14 (uncooperativeness)
Excitement	zPANNSP4 (excitement) + zPANNSP5 (grandiosity) + zBPRS8 (grandiosity) + zBPRS17 (excitement)
Mannerism	zPANNSG5 + zBPRS7 (both mannerism and posturing)
Formal thought disorders	zPANNSP2 (conceptual disorganization) + item 5 of the PANNS negative subscale (PANNSN5: difficulty in abstract thinking) + zBPRS4 (item 4 of the BPRS or conceptual disorganization)
Psychomotor retardation	*z* score of HDRS item 8 (HDRS8: psychomotor retardation: slowness of thought and speech, decreased motor activity, impaired inability to concentrate) + zPANSSG7 (reduction in motor activity as reflected in slowing or lessening of movements and speech, diminished responsiveness to stimuli and reduced body tone) + zBPRS13 (reduction in energy level evidenced in slowed movements)
Executive functions	zOTS_PSOFC + zSWM_STR + zSWM_BE
NOX/PRO TRYCAT	Ratio of noxious TRYCATs/generally more protective TRYCATs computed as *z* score of PA (zPA) + zXA + zOHK − zAA − zKA
Immune activation index	*z* Interleukin-10 (IL10) + *z* macrophage inflammatory protein + *z* soluble IL-1 receptor antagonist

PANNS, Positive and Negative Syndrome Scale; *BPRS*, Brief Psychiatric Rating Scale (BPRS); *HDRS*, Hamilton Depression Rating Scale; zOTS_PSOFC: One touch stockings of Cambridge probability solved on first choice; *zSWM_STR*, spatial working memory, strategy; *zSWM_BE*, SWM between errors; *PA*, picolinic acid; *XA*, xanthurenic acid; *OHK*, 3-hydroxy kynurenine; *AA*, anthranilic acid; *KA*, kynurenic acid

SWM strategy (SWM_STR) and SWM between errors (SWM_BE), to probe task strategy, executive working memory ability, self-monitoring ability, and maintenance of data in the visuospatial sketchpad. Table 2 shows the computation of the *z* unit weighted score reflecting executive functions. Finally, we used DSM-IV-TR criteria to make the diagnosis of nicotine dependence. Body mass index (BMI) was computed as: body weight (kg) / length (m^2).

Assays

In patients and controls, fasting blood was sampled at 8:00 a.m. for the assay of IgA responses to paracellular, vascular, and transcellular pathway proteins (see Table 1), IgM antibody levels to MDA, IgA responses to TRYCATs, and IL-10, sIL-1RA, MIP-1α, and CCL-11 (eotaxin) levels. Different proteins/peptides such as claudin-5, occludin, E-cadherin, talin, vinculin, EIF (keratin), PLVAP, and epithelial and endothelial adherent junctions (β-catenin) were purchased from Bio-Synthesis Inc. (Lewisville, TX, USA) and Abcam (Cambridge, MA, USA). Actin was obtained from Sigma-Aldrich (St Louis, MO, USA). For determination of antibody levels, proteins and peptides at a concentration of 1 mg/mL were dissolved in 0.01 M phosphate buffered saline (PBS) buffer at pH 7.4 and diluted 1:100 in 0.1 M carbonate buffer at pH 9.5; 100 μL of each diluted antigen was added to each well of the costar microtiter plate. Plates were incubated overnight at 4 °C and then washed three times with 200 μL of 0.01 M PBS containing 0.05% Tween 20 at pH 7.4. After washing, 200 μL of 5% bovine serum albumin (BSA) was added to each well to prevent nonspecific binding of the antibody to the plate. Plates were washed, and then 100 μL of serum diluted at 1:50 for IgA detection in serum diluent was added to duplicate wells coated with each antigen. Plates were incubated for an additional 1 h at room temperature. Plates were washed again for five times with Tris-buffered saline (TBS)-Tween. Alkaline phosphatase-labeled anti-human IgA diluted at 1:200 was added to all wells and incubated again for 1 h at room temperature. Following the addition of 100 μL of paranitrophenylphosphate at a concentration of 1 mg/mL in diethanolamine buffer, the reaction was stopped 30 min later with 75 μL of 1 N NaOH, and the samples were read by an ELISA reader; the optical densities were recorded. Several wells coated with nonspecific proteins such as human serum albumin (HAS) and rabbit serum albumin were used as controls for detecting the ELISA background. Sera from healthy subject were used as controls and sera from patients with autoimmunity with moderate and high titers of IgA antibodies were used as calibrator and positive controls for the calculation of ELISA indices using the following formula: Antibody ELISA index = OD of tested Specimen − OD of blank / OD of Calibrator − OD of blank. The variability in the duplicate test results was less than 7%. The optical density (OD) values were transformed into *z* scores which we employed in statistical analyses. *z* unit weighted composite scores were computed to obtain indices of paracellular, vascular, and transcellular pathways (see Table 1).

We used an enzyme-linked immunosorbent assay to measure IgM levels directed against conjugated MDA (Daverat et al. 1989; Boullerne et al. 1996; Amara et al. 1995). MDA was linked to fatty acid free-BSA as described in the abovementioned studies. The detection of IgM autoantibodies to the conjugates was performed by indirect ELISA tests (Faiderbe et al. 1992; Boullerne et al. 2002). Briefly, polystyrene 96-well plates (NUNC) were coated with 200 μL solution containing the conjugates or BSA in 0.05 M carbonate buffer at pH 9.6. Well plates were incubated at 4 °C for 16 h under agitation. Then, a 200-μL of blocking solution (PBS, 2.5 g/L BSA) was added for 1 h and placed at 37 °C. Following three washes with PBS, plates were filled up with 100 μL of sera diluted at 1:1000 in blocking buffer A (PBS, 0.05% Tween 20, 10% glycerol, 2.5 g/L BSA, 1 g/L BSA-G) and incubated at 37 °C for 2 h. After three washes with PBS–0.05% Tween 20, plates were incubated at 37 °C for 1 h with peroxidase-labeled anti-human IgM secondary antibodies diluted, respectively, at 1: 15,000, in the blocking buffer (PBS, 0.05% Tween 20, 2.5 g/L BSA). They were then washed three times with PBS–0.05% Tween 20 and incubated with the detection solution for 10 min in the dark. Chromogen detection solution was used for the peroxidase assay at 8% in 0.1 M acetate and 0.01 M phosphate buffer (pH 5.0) containing 0.01% H_2O_2. The reaction was stopped with 25 μL 2-N HCl. ODs were measured at 492 nm using a multiscan spectrophotometer. All assays were carried out in duplicate. The intra-assay coefficients of variation (CV) were < 6%.

The assays of IgA responses to conjugated TRYCATs were performed as described previously (Duleu et al. 2010; Roomruangwong et al. 2017, 2018a). The TRYCATs were dissolved in 200 μL dimethylsulfoxide (DMSO) (Acros). BSA (ID Bio) was dissolved in 3 mL 2-morpholinoethanesulfonic acid monohydrate (MES) buffer 10^{-1} M at pH = 6.3 (Acros). The TRYCATs were then mixed with the BSA solution and supplemented with 15 mg *N*-hydroxysuccinimide (Sigma) and 1-(3-dimethylaminopropyl)-3-ethylcarbodiimide (Acros) as coupling agents. The conjugates were synthesized by linking 3-OH-kynurenine (3HK, Sigma), kynurenic acid (KA, Acros), quinolinic acid (QA, Acros), anthranilic acid (AA, Acros), xanthurenic acid (XA, Akros), and picolinic acid (PA, Akros) to 20 mg BSA. The coupling reaction proceeded at 37 °C for 1 h in the dark. The coupling was stopped by adding 100 mg hydroxylamine (Sigma-Aldrich) per conjugate. Protein conjugates were dialyzed with 10^{-1} M NaCl solution for 72 h, and the bath solution was changed at least four times per day. The conjugated TRYCATs and BSA concentrations were evaluated by spectrophotometry. The coupling ratio of

each conjugate was determined by measuring the concentration of TRYCATs and BSA at 310–330 and 280 nm, respectively. ELISA tests were used to determine plasma titers of IgA. Toward this end, polystyrene 96-well plates (NUNC) were coated with 200 μL solution containing 10–50 μg/mL TRYCAT conjugates in 0.05 M carbonate buffer (pH = 9.6). Well plates were incubated under agitation at 4 °C for 16 h. Then, 200 μL blocking buffer A (PBS, 2.5 g/L BSA) was applied and all samples were incubated at 37 °C for 1 h. Well plates were washed with PBS solution and filled up with 100 μL serum diluted 1:130 in blocking buffer and incubated at 37 °C for 1 h and 45 min. Well plates were washed three times with PBS, 0.05% Tween 20 and incubated with peroxidase-labeled goat anti-human IgA (SouthernBiotech) antibodies at 37 °C for 1 h. The goat anti-human IgA antibody was diluted at 1:10,000 in blocking buffer (PBS, 2.5 g/L BSA). Plates were then washed three times with PBS, 0.05% Tween 20. Fifty microliters of TMB substrate (3,3′,5,5′-tetramethylbenzidine, SouthernBiotech) was added and incubated for 10 min in the dark. The reaction was stopped using 50 μL of TMB stop solution (SouthernBiotech). ODs were measured at 450 nm using Varioskan Flash (Thermo Scientific). All assays were carried out in one and the same run by the same operator who was blind to all clinical results. All assays were carried out in duplicate. The analytical intra-assay CV values were < 7%. Table 2 shows the computation of the noxious/more protective (NOX/PRO) TRYCAT ratio (Kanchanatawan et al. 2018a).

For the assays of CCL-11, sIL-1RA, IL-10, and MIP-1α (Sirivichayakul et al. 2018), 50 μL of serum (1:2 dilution in calibrator diluents) was mixed with 50 μL of microparticle cocktail containing these cytokines and chemokines (R&D Systems, Inc., Minneapolis, MN, USA) per well of a 96-well plate provided by the manufacturer and incubated for 2 h at room temperature on a shaker at 800 rpm. The mixture was then washed three times with wash buffer, and 50 μL diluted biotin antibody cocktail was added and then incubated for 1 h. Wells were washed three times before another 50 μL of diluted streptavidin-PE was added and further incubated for 30 min. Finally, wells were washed three times and 100 μL of wash buffer was added and left at room temperature for 2 min before being read with Bio-Plex® 200 System (Bio-Rad Laboratories, Inc.). The intra-assay CV values were < 7.0%. The least detectable dose was 1.82 pg/mL for eotaxin, 1.58 pg/mL for MIP-1, 5.98 pg/mL for IL-1RA, and 0.4 pg/mL for IL-10. We computed an immune activation index (see also Table 2) as z score of interleukin-10 (zIL-10) + zMIP-1α + zsIL-1RA (Sirivichayakul et al. 2018, 2019).

Statistical Analysis

We employed analysis of contingency tables (χ^2 tests) to check associations between two categorical variables and analysis of variance (ANOVA) to check differences in continuous variables between groups. We inspected correlation matrices to check associations between sets of continuous variables using Pearson's product moment and Spearman's rank order correlation coefficients. Multinomial logistic regression analysis was used to assess the significant predictors of deficit and nondeficit schizophrenia and controls while adjusting for extraneous variables and other biomarkers. Multivariate general linear model (GLM) analysis was used to check the effects of extraneous variables on the IgA responses. Results of tests for between-subject effects were p-corrected for false discovery rate (FDR) (Benjamini and Hochberg 1995). We employed multiple regression analysis to delineate the biomarkers that best predict specific symptom domains and neurocognitive test scores. We checked results of regression analyses for multicollinearity using tolerance and VIF values. We also reran the analyses using 1000 bootstraps and report the bootstrapped results if there would be differences between the analyses with and without bootstrapping. We employed receiver operating characteristics (ROC) analysis to compute the area under the ROC curve (AUC) and computed the AUC after 2000 bootstraps. We also computed composite scores reflecting the PARA/TRANS ratio (based on the IgA responses to the proteins) and split the study group into two subgroups based on the 0.666 percentile-split method. Eotaxin and IgM to MDA were processed in Ln transformations in order to normalize their data distribution. Tests were two tailed and a p value of 0.05 was used for statistical significance. All abovementioned statistical analyses were performed using IBM SPSS Windows version 25.

Results

Demographic Data

Table 3 shows the basic demographic data in controls and both groups of schizophrenia. There were no significant differences in age, education, and nicotine dependence between the three subgroups. There were somewhat more males in the schizophrenia subgroups than in the controls. BMI was lower in patients with deficit schizophrenia than in nondeficit schizophrenia. SDS, SANS, and PANSS negative subscale scores were higher in deficit schizophrenia than in nondeficit schizophrenia and controls. PANSS positive subscale score was not significantly different between both schizophrenia subgroups.

Biomarkers and Schizophrenia Categories

Table 4 displays the results of different multinomial logistic regression analyses with diagnosis (three groups) as dependent variables and the paracellular, vascular, and transcellular

Table 3 Demographic and clinical data in normal controls and schizophrenic patients with and without the deficit syndrome

Variables	Controls[A]	Nondeficit schizophrenia[B]	Deficit schizophrenia[C]	$F/\Psi/\chi^2$	*df*	ρ
Age (years)	37.4 (12.8)	41.3 (10.8)	41.1 (11.4)	1.41	2/116	0.248
Sex (F/M)	30/10[B, C]	18/22[A]	19/20[A]	8.67	2	0.013
BMI (kg/m^2)	24.0 (4.3)	26.0 (5.2)[C]	22.8 (4.7)[B]	4.41	2/111	0.014
Education (years)	14.3 (4.9)	12.8 (4.1)	11.9 (4.2)	2.82	2/116	0.064
Nicotine dependence (N/Y)	38/2	36/4	38/1	$\Psi = 0.131$	–	0.358
SDS	0.0	2.1 (1.6)	11.8 (4.4)	KWT	–	< 0.001
SANS	0.5 (1.7)[B, C]	17.1 (10.6)[A, C]	53.3 (19.2)[A, B]	KWT	–	< 0.001
PANSS+	7.0 (0.0)[B, C]	13.6 (8.2)[A]	15.3 (6.9)[A]	KWT	–	< 0.001
PANSS−	7.0 (0.0)[B, C]	10.9 (4.0)[A, C]	27.8 (7.4)[A, B]	KWT	–	< 0.001

All results are shown as mean (SD)

KWT, results of the Kruskal–Wallis test; *BMI*, body mass index; *SDS*, Schedule for the Deficit Syndrome; *SANS*, Scale for the Assessment of Negative Symptoms; *PANSS+/−*, positive and negative subscales of the Positive and Negative Syndrome Scale

[A, B, C] Pairwise comparisons among the three subgroups (tested at $p < 0.05$)

biomarkers as explanatory variables while controlling for age, sex, BMI, and education. The same analyses were also rerun with CCL-11, IgM to MDA, and the immune activation index as additional explanatory variables to assess whether the IgA levels had an effect above and beyond these three biomarkers. We found a strong association between the paracellular index and diagnoses with an effect size of 0.731 for the total model, 0.633 without the paracellular index, and 0.089 for the

Table 4 Results of multinomial logistic regression analysis with diagnoses as dependent variables and IgA responses to proteins of the paracellular (PARA), transcellular (TRANS), and vascular pathways as explanatory variables. Diagnostic groups are healthy controls (HC) and patients with (Def) and without (Non-Def) deficit schizophrenia

Dependent variables	Explanatory variables	Wald	*df*	*p*	OR	95% CI intervals	Nagelkerke (of model)* χ^2, *df*, *p* (of explanatory variable)*
Non-Def/HC	Paracellular	1.78	1	0.182	0.62	0.31–1.25	0.731
Def/HC	Paracellular	8.09	1	0.004	2.92	1.40–6.12	$\chi^2 = 21.82$, $df = 2$, $p < 0.001$
Def/Non-Def	Paracellular	15.21	1	< 0.001	4.68	2.16–10.17	
Non-Def/HC	Transcellular	3.00	1	0.083	0.55	0.28–1.08	0.665
Def/HC	Transcellular	0.281	1	0.600	0.83	0.40–1.69	$\chi^2 = 3.70$, $df = 2$, $p < 0.001$
Def/Non-Def	Transcellular	1.59	1	0.207	1.51	0.80–2.85	
Non-Def/HC	Vascular	2.19	1	0.139	0.60	0.31–1.18	0.705
Def/HC	Vascular	4.17	1	0.041	1.97	1.03–3.78	$\chi^2 = 14.15$, $df = 2$, $p < 0.001$
Def/Non-Def	Vascular	11.50	1	0.001	3.26	1.65–6.46	
Non-Def/HC	Gut barrier	2.88	1	0.089	0.54	0.26–1.10	0.734
Def/HC	Gut barrier	7.17	1	0.007	2.69	1.30–5.53	$\chi^2 = 22.68$, $df = 2$, $p < 0.001$
Def/Non-Def	Gut barrier	15.80	1	< 0.001	4.99	2.26–11.03	
Non-Def/HC	BBB	2.38	1	0.123	0.58	0.29–4.41	0.727
Def/HC	BBB	6.62	1	0.010	2.62	1.26–5.50	$\chi^2 = 20.79$, $df = 2$, $p < 0.001$
Def/Non-Def	BBB	14.74	1	< 0.001	4.56	2.10–9.90	
Non-Def/HC	PARA/TRANS	0.60	1	0.438	1.42	0.58–3.46	0.828
Def/HC	PARA/TRANS	22.21	1	< 0.001	21.72	6.04–78.15	$\chi^2 = 70.75$, $df = 2$, $p < 0.001$
Def/Non-Def	PARA/TRANS	19.03	1	< 0.001	15.28	4.49–52.01	
Non-Def/HC	IgM MDA	5.41	1	0.020	4.98	1.29–19.28	0.886
	Immune activation	8.65	1	0.003	9.51	2.12–42.70	$\chi^2 = 181.03$, $df = 18$, $p < 0.001$
	Eotaxin	11.44	1	0.001	69.57	5.96–812.65	
	IgA NOX/PRO	7.08	1	0.008	11.21	1.89–66.50	
Def/HC	Immune activation	6.11	1	0.013	9.68	1.60–58.53	
	Eotaxin	6.08	1	0.014	23.13	1.90–280.96	
	IgA NOX/PRO	7.04	1	0.008	12.44	1.93–80.15	
	PARA/TRANS	8.52	1	0.004	9.30	1.93–80.15	
Def/Non-def	IgM MDA	8.91	1	0.003	0.051	0.01–0.36	
	IgA Gram− bacteria	6.95	1	0.008	3.07	1.33–7.07	
	PARA/TRANS	10.03	1	0.002	7.71	2.18–27.31	

All regression analyses are adjusted for age, sex, education, and IgM to malondialdehyde, CCL-11, and the immune activation index

OR, odds ratio; *95% CI*, 95% confidence intervals with upper and lower limits

* Nagelkerke value of the model; χ^2 values of the explanatory variable(s)

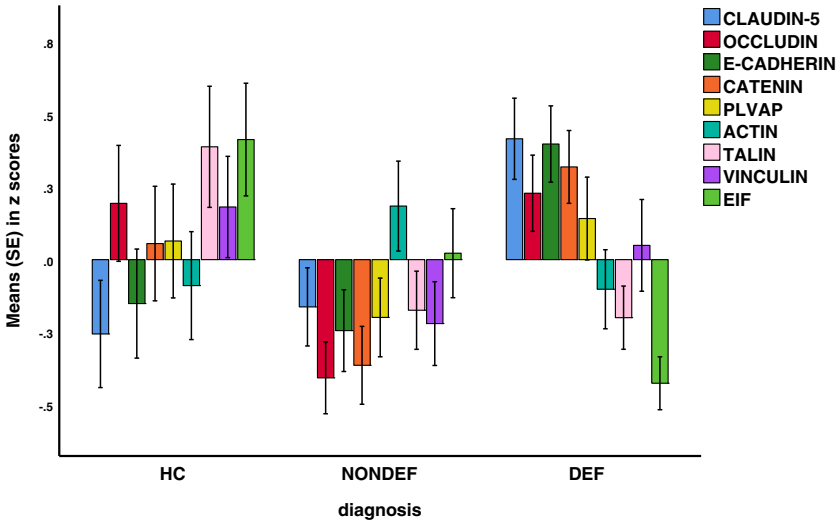

Fig. 1 Mean IgA responses (in z scores ± SE) to paracellular, transcellular, and vascular proteins in patients with deficit schizophrenia (DEF), nondeficit schizophrenia (NONDEF), and healthy controls (HC). PLVAP, plasmalemma vesicle-associated protein; EIF, epithelial intermediate filament

paracellular index. A higher paracellular index significantly predicted deficit schizophrenia versus controls and nondeficit schizophrenia, while there were no differences between controls and nondeficit schizophrenia. Figures 1 and 2 show the mean z scores of the paracellular, transcellular, and vascular index proteins in the three study groups. IgA responses to claudin-5 ($\chi^2 = 18.59$, $df = 2$, $p < 0.001$), occludin ($\chi^2 = 24.87$, $df = 2$, $p < 0.001$), E-cadherin ($\chi^2 = 22.34$, $df = 2$, $p < 0.001$), and β-catenin ($\chi^2 = 16.70$, $df = 2$, $p < 0.001$) were significantly associated with the diagnostic groups (after p correction for FDR). Higher claudin-5, E-cadherin, and β-catenin were significantly associated with deficit schizophrenia versus controls and nondeficit schizophrenia. Higher occludin was significantly associated with deficit schizophrenia versus nondeficit schizophrenia and was lower in the latter than in the controls. We could not detect a significant association between the transcellular index and the diagnostic groups, while after FDR p correction, talin ($p = 0.043$) and EIF ($p = 0.043$) showed a significant association with the diagnostic groups. Lowered IgA levels to talin were associated with nondeficit ($p = 0.023$) and deficit ($p = 0.021$) schizophrenia versus controls, whereas lower EIF was associated with deficit schizophrenia as compared with controls ($p = 0.001$) and nondeficit schizophrenia ($p = 0.045$) (see also Fig. 1). Table 4 and Figs. 1 and 2 show that increased vascular, gut barrier, and BBB indices were significantly associated with deficit schizophrenia versus nondeficit schizophrenia and controls, while there were no significant differences between nondeficit schizophrenia and controls.

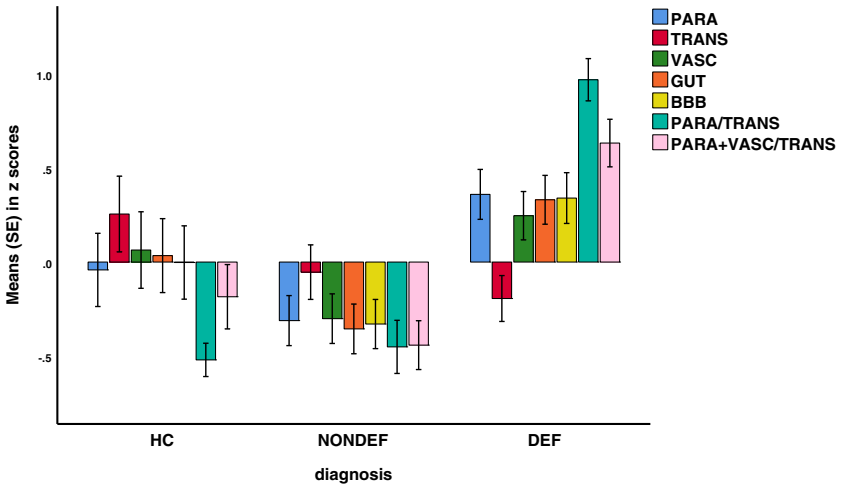

Fig. 2 Mean indices (in z scores ± SE) of the paracellular (PARA), transcellular (TRANS), and vascular (VASC) pathways and gut (GUT) and blood brain (BBB) barriers and the PARA(+VASC)/TRANS ratios in patients with deficit schizophrenia (DEF), nondeficit schizophrenia (NONDEF), and healthy controls (HC). PARA: includes occludin, claudin-5, E-cadherin, and β-catenin. TRANS: includes talin, actin, vinculin, and epithelial intermediate filament. Vascular: includes β-catenin and plasmalemma vesicle-associated protein. GUT: gut barrier index includes E-cadherin, occludin, and β-catenin. BBB: blood brain barrier index includes claudin-5, occludin, and β-catenin

Table 5 Sociodemographic, clinical, and biomarker data in schizophrenia (SCZ) patients with a higher versus lower paracellular/transcellular (PARA/TRANS) pathway ratio as compared with healthy controls (HC)

Variables	HC ($n = 40$)^{A}	IgA PARA/TRANS < 0.666% ($n = 50$)^{B}	IgA PARA/TRANS ≥ 0.666% ($n = 26$)^{C}	$F/\chi^2/\Psi$	*df*	*p*
Age (years)	37.4 (12.8)	40.8 (10.7)	42.08 (12.0)	1.52	2/116	0.223
Sex (M/F)	10/30^{B}	30/23^{A}	12/14	8.64	2	0.013
Education (years)	14.3 (4.9)	12.4 (4.1)	12.2 (4.3)	2.46	2/116	0.090
Single/married/separated	23/14/3	30/9/5	21/2/2	$\Psi = 0.26$	–	0.101
Nicotine dependence (N/Y)	38/2	48/5	26/0	$\Psi = 0.16$	–	0.236
Body mass index (kg/m^2)	24.0 (4.3)	25.3 (5.1)	22.7 (5.1)	2.45	2/111	0.091
Number of psychotic episodes	–	3.35 (2.66)^{C}	2.77 (3.04)^{B}	0.66	1/72	0.420
Age at onset (years)	–	24.8 (9.2)	28.5 (8.9)	2.64	1/73	0.108
SDS	0.0 (0.0)$^{B, C}$	4.8 (5.5)$^{A, C}$	10.8 (4.3)$^{A, B}$	50.15	2/114	< 0.001
SANS	0.5 (1.7)$^{B, C}$	27.8 (22.7)$^{A, C}$	49.4 (19.26)$^{A, B}$	62.79	2/115	< 0.001
PANSS negative	7.0 (0.0)$^{B, C}$	15.9 (9.6)$^{A, C}$	25.9 (8.7)$^{A, B}$	49.06	2/115	< 0.001
PANSS positive	7.0 (0.0)$^{B, C}$	13.8 (7.7)^{A}	15.7 (7.2)^{A}	19.89	2/115	< 0.001
Psychosis (*z* score)	− 0.820 (0.0)$^{B, C}$	0.202 (0.991)$^{A, C}$	0.843 (0.890)$^{A, B}$	38.41	2/115	< 0.001
Hostility (*z* score)	− 0.595 (0.0)$^{B, C}$	0.221 (1.088)^{A}	0.461 (1.191)^{A}	13.25	2/115	< 0.001
Excitement (z score)	− 0.809 (0.0)$^{B, C}$	0.132 (0.967)$^{A, C}$	0.901 (0.862)$^{A, B}$	41.60	2/116	< 0.001
Mannerism (z score)	− 0.737 (0.0)$^{B, C}$	0.245 (0.986)^{A}	0.655 (1.152)^{A}	24.86	2/115	< 0.001
PMRI (*z* score)	− 0.772 (0.143)$^{B, C}$	0.124 (0.996)$^{A, C}$	0.944 (0.871)$^{A, B}$	38.20	2/115	< 0.001
FTD (*z* score)	− 0.761 (0.0)$^{B, C}$	0.233 (1.031)$^{A, C}$	0.666 (0.985)$^{A, B}$	27.10	2/115	< 0.001
Nondeficit/deficit SCZ	–	38/15^{C}	2/24^{B}	28.59	1	< 0.001
IgM MDA (*z* score)	0.275 (0.821)^{C}	0.060 (1.043)^{C}	− 0.487 (1.003)$^{A, B}$	4.92	2/114	0.009
IgA Gram-negative (z score)	− 0.017 (0.885)	− 0.209 (1.043)^{C}	0.445 (0.975)^{B}	3.89	2/114	0.023
Immune activation (*z* score)	− 0.674 (0.857)$^{B, C}$	0.441 (0.921)^{A}	0.116 (0.828)^{A}	18.61	2/116	< 0.001
CCL-11 or eotaxin (pg/mL)*	129.6 (54.1)$^{B, C}$	216.3 (106.3)^{A}	202.0 (91.0)^{A}	18.27	2/116	< 0.001
IgA NOX/PRO (*z* score)	− 0.695 (0.655)$^{B, C}$	0.015 (0.813)$^{A, C}$	1.010 (0.926)$^{A, B}$	36.69	2/116	< 0.001
Verbal fluency test	26.6 (6.3)$^{B, C}$	19.1 (6.6)^{A}	16.8 (6.0)^{A}	23.33	2/116	< 0.001
Word list (WL) memory	22.1 (4.4)$^{B, C}$	17.4 (4.9)^{A}	15.7 (5.7)^{A}	16.08	2/116	< 0.001
WL true recall	8.1 (1.8)$^{B, C}$	6.6 (2.1)$^{A, C}$	5.4 (2.3)$^{A, B}$	14.03	2/116	< 0.001
Executive functions	− 0.711 (0.942)$^{B, C}$	0.236 (0.855)^{A}	0.584 (0.730)^{A}	21.33	2/115	< 0.001

All results are shown as mean (±SD)

$F/\chi^2/\Psi$, results of analyses of variance (F) or analyses of contingency (χ^2) or Ψ coefficient; *BMI*, body mass index; *SDS*, total score on the Schedule for Deficit Syndrome; *SANS*, Scale for the Assessment of Negative Symptoms; *PANSS*, total score on the Positive and Negative Syndrome Scale; *PMRI*, psychomotor retardation index; *FTD*, formal thought disorders see Table 2 for explanation; *IgM MDA*, IgM antibodies to malondialdehyde; *IgA Gram-negative bacteria*, composite score computed as sum of all *z* transformations of the IgA responses to Gram-negative bacteria; *Immune activation index*, composite score computed as sum of all *z* transformations of three cytokines/chemokines; *IgA NOX/PRO*, IgA responses to noxious/protective tryptophan catabolites

$^{A, B, C}$ Pairwise comparisons among the three subgroups (tested at $p < 0.05$)

Entering the PARA/TRANS ratio in the regression improved the Nagelkerke value from 0.633 to 0.828, while the effect size of this ratio was 0.515. An increased PARA/TRANS ratio was significantly associated with deficit versus nondeficit schizophrenia and controls. The ROC curve of the PARA/TRANS ratio for deficit schizophrenia (versus nondeficit schizophrenia + controls) was 0.952 (± 0.019) ($p < 0.001$, 95% confidence intervals 0.915–0.988), while the bootstrapped AUC (2000 bootstraps) was 0.936 (95% confidence intervals 0.893–0.974).

Finally, we have also examined whether the PARA/TRANS ratio has a significant impact beyond and above that of the biomarkers NOX/PRO TRYCAT ratio, IgA Gram-negative bacteria, CCL-11, immune activation index, and IgM MDA.

We found that these four biomarkers were significantly associated with the diagnostic groups with an effect size of 0.886 (see last regression of Table 4): nondeficit schizophrenia was discriminated from controls by increased IgM to MDA, immune activation index, CCL-11, and IgA NOX/PRO TRYCAT ratio. Deficit schizophrenia was best discriminated from controls by increased PARA/TRANS ratio, immune activation index, CCL-11, and IgA TRYCAT ratio. Deficit schizophrenia was best discriminated from nondeficit schizophrenia by increased PARA/TRANS ratio and increased IgA to Gram-negative bacteria and lowered IgM to MDA.

Characteristics of Increased IgA PARA/TRANS Ratio

Based on the strong impact of the IgA PARA/TRANS ratio on diagnostic classifications, we have examined the clinical, neurocognitive, and biomarker characteristics of patients with schizophrenia with a PARA/TRANS ratio that was higher than the 0.666 percentile versus those with a lower ratio and normal controls. Table 5 shows the results of different ANOVAs and χ^2 tests examining the differences between these three study samples. We found no significant differences in age, education, marital status, nicotine use, and BMI between the three study groups. There were somewhat more females in the schizophrenia group with lower PARA/TRANS values than in controls. Age at onset of schizophrenia and number of psychotic episodes were not significantly different between both schizophrenia subgroups. The scores on the SDS, SANS, PANSS negative, psychosis, excitement, PMRI, and FTD were significantly higher in patients with a higher PARA/TRANS ratio than in the other patients and controls. IgM MDA and WL true recall were significantly lower and IgA responses to the NOX/PRO TRYCAT ratio significantly higher in patients with a higher PARA/TRANS ratio as compared with the other two study groups. IgA levels to Gram-negative bacteria were significantly higher in patients with an increased PARA/TRANS ratio, while PANNS positive, hostility, mannerism, immune activation index, and CCL-11 were significantly higher in schizophrenia than in controls. VFT, WLM, and executive functions were significantly lower in schizophrenia than in controls, although there was a trend toward lower test scores in patients with a high PARA/TRANS ratio.

Effects of Extraneous Variables

Multivariate GLM analysis showed no significant effects of gender ($F = 1.15$, $df = 9/97$, $p = 0.336$), age ($F = 1.91$, $df = 9/97$, $p = 0.059$), and education ($F = 0.60$, $df = 9/97$, $p = 0.798$) on the nine IgA responses to paracellular, transcellular, and vascular proteins. There was a significant effect of BMI on the IgA values and tests for between-subject effects, and parameter estimates showed a significant positive effect of BMI on talin ($F = 8.61$, $df = 1/105$, $p = 0.004$), vinculin ($F = 7.93$, $df = 1/105$, $p = 0.006$), and actin ($F = 6.94$, $df = 1/105$, $p = 0.010$). There was no significant effect of nicotine dependence on the nine IgA values ($F = 1.56$, $df = 9/96$, $p = 0.138$). Another multivariate GLM analysis did not reveal any significant effects (even at the $p = 0.05$ level without FDR p correction) of use of risperidone ($F = 1.23$, $df = 9/93$, $p = 0.289$; $n = 34$), clozapine ($F = 0.59$, $df = 9/93$, $p = 0.802$; $n = 9$), haloperidol ($F = 0.95$, $df = 9/93$, $p = 0.487$; $n = 11$), perphenazine ($F = 0.85$, $df = 9/93$, $p = 0.570$; $n = 21$), antidepressants ($F = 0.66$, $df = 9/93$, $p = 0.747$; $n = 26$), mood stabilizers ($F = 1.23$, $df = 9/93$, $p = 0.287$; $n = 13$), and anxiolytics/hypnotics ($F = 0.93$, $df = 9/93$, $p = 0.505$; $n = 29$) on the nine IgA responses.

Prediction of SCZ Symptomatology Using Biomarkers

Table 6 shows the predictions of symptom domains using the IgA PARA/TRANS ratio, IgA to Gram-negative bacteria (or IgA to *Klebsiella pneumoniae* or *Pseudomonas aeruginosa*), CCL-11, immune activation index, IgM to MDA, and the NOX/PRO TRYCAT ratio. Table 6 regression #1 shows that 53.4% of the variance in the SDS score was explained by IgA PARA/TRANS and immune activation index (both positively) and IgM MDA and education (both negatively). Table 6 regression #2 shows that 44.7% of the variance in the PANSS negative subscore was explained by IgA PARA/TRANS and immune activation index (both positively) and education (negatively). Regression #3 shows that 49.9% of the variance in the SANS score was explained by IgA PARA/TRANS, immune activation, and CCL-11 (all positively). Regression #4 shows that 45.4% of the variance in the PMRI is explained by the regression on the PARA/TRANS ratio, CCL-11, immune activation, and IgA *K. pneumoniae*. Around 26.6% of the variance in psychotic symptoms was explained by two biomarkers, namely the PARA/TRANS and immune activation ratios. Hostility was best explained by the regression on the PARA/TRANS ratio, immune activation, and IgA *P. aeruginosa.* We found that (regression #7, 8, and 9) a large part of the variances in excitation (36.1%), mannerism (23.0%), and FTD (21.1%) scores were explained by the PARA/TRANS ratio, immune activation, and CCL-11 (all positive). The PARA/TRANS ratio was also a significant predictor of neurocognitive tests including VFT, WLM, WL true recall, and executive functions together with education, age, or sex and other biomarkers.

Prediction of Indices of BBB Permeability and Bacterial Translocation

Table 7 regression #1–2 show the outcome of regression analyses with IgA to claudin-5 as dependent variable and selected biomarkers as explanatory variables, namely IgA E-cadherin and Gram-negative bacteria (as biomarkers of leaky gut) and the immune activation index, CCL-11, and NOX/PRO

Table 6 Results of hierachical multiple regression analyses with severity of schizophrenia symptom domains as dependent variables and IgA responses to paracellular, transcellular, and vascular pathway proteins and other biomarkers as explanatory variables

Dependent variables	Explanatory variables	BE (SE)	*t*	*p*	R^2	Model *F*	*df*	*p*
#1. SDS	Model				0.534	31.54	4/110	< 0.001
	PARA/TRANS	2.742 (0.411)	6.68	< 0.001				
	Immune activation	1.451 (0.383)	3.79	< 0.001				
	IgM MDA	− 1.174 (0.405)	− 2.90	0.005				
	Education	− 0.238 (0.084)	− 2.83	0.006				
#2. PANSS negative	Model				0.4474	30.13	3/112	< 0.001
	PARA/TRANS	5.671 (0.734)	7.73	< 0.001				
	Immune activation	2.105 (0.730)	2.88	0.005				
	Education	− 0.435 (0.162)	− 2.67	0.009				
#3. SANS	Model				0.499	36.84	3/111	< 0.001
	PARA/TRANS	13.339 (1.763)	7.57	< 0.001				
	Immune activation	7.217 (1.773)	4.07	< 0.001				
	CCL-11	5.053 (1.842)	2.74	0.007				
#4. PMRI	Model				0.454	22.86	4/110	< 0.001
	PARA/TRANS	0.436 (0.076)	5.70	< 0.001				
	CCL-11	0.218 (0.077)	2.82	0.006				
	Immune activation	0.221 (0.074)	2.99	0.003				
	IgA *K. pneumoniae*	0.178 (0.078)	2.29	0.024				
#5. Psychotic symptoms	Model				0.266	20.28	2/112	< 0.001
	PARA/TRANS	0.410 (0.082)	4.99	< 0.001				
	Immune activation	0.269 (0.081)	3.32	0.001				
#6. Hostility	Model				0.162	7.14	3/111	< 0.001
	Immune activation	0.248 (0.086)	2.87	0.005				
	PARA/TRANS	0.259 (0.090)	2.88	0.005				
	IgA *P. aeruginosa*	− 0.206 (0.090)	− 2.28	0.025				
#7. Excitation	Model				0.361	21.08	3/112	< 0.001
	PARA/TRANS	0.472 (0.076)	6.20	< 0.001				
	Immune activation	0.190 (0.078)	2.45	0.016				
	CCL-11	0.171 (0.081)	2.12	0.036				
#8. Mannerism	Model				0.230	11.06	3/111	< 0.001
	PARA/TRANS	0.296 (0.086)	3.45	0.001				
	Immune activation	0.227 (0.086)	2.64	0.010				
	CCL-11	0.180 (0.090)	2.01	0.047				
#9. FTD	Model				0.211	9.92	3/111	< 0.001
	PARA/TRANS	0.278 (0.081)	3.42	0.001				
	Immune activation	0.182 (0.082)	2.23	0.028				
	CCL-11	0.169 (0.085)	1.99	0.049				
#10. VFT	Model				0.390	13.56	5/110	< 0.001
	Education	0.440 (0.135)	3.27	0.001				
	PARA/TRANS	− 2.004 (0.567)	− 3.54	0.001				
	Immune activation	− 1.838 (0.591)	− 3.11	0.002				
	CCL-11	− 1.876 (0.665)	− 2.82	0.006				
	Sex	− 2.683 (1.203)	− 2.23	0.028				
#11. WLM	Model				0.376	22.46	3/112	< 0.001
	Education	0.499 (0.093)	5.36	< 0.001				
	Immune activation	− 1.502 (0.417)	− 3.60	< 0.001				
	PARA/TRANS	− 1.396 (0.416)	− 3.36	0.001				
#12. WL true recall	Model				0.385	17.40	4/111	< 0.001
	Immune activation	− 0.677 (0.176)	− 3.84	< 0.001				
	Education	0.145 (0.038)	3.80	< 0.001				
	PARA/TRANS	− 0.639 (0.170)	− 3.76	< 0.001				
	Sex	0.783 (0.351)	2.23	0.028				
#13. Executive functions	Model				0.460	23.46	4/110	< 0.001
	Education	− 0.095 (0.380)	− 4.64	< 0.001				
	Age	0.076 (0.016)	4.40	< 0.001				
	Immune activation	0.231 (0.070)	3.28	0.001				
	PARA/TRANS	0.185 (0.071)	2.59	0.011				

All dependent and explanatory variables were entered as *z* scores (the IgM MDA data were first Ln transformed)

SDS, total score on the Schedule for Deficit Syndrome; *PANSS*, total score on the Positive and Negative Syndrome Scale; *SANS*, Scale for the Assessment of negative Symptoms; *PMRI*, psychomotor retardation index; *FTD*, formal thought disorders, see Table 2 for calculation; *IgM MDA*, IgM responses to malondialdehyde; *PARA/TRANS*, paracellular/transcellular pathway ratio; *IgM Gram-negative bacteria*, composite score computed as sum of all z transformations of the IgA responses to Gram-negative bacteria

Table 7 Results of multiple regression analyses with IgA responses to claudin-5 and IgA to Gram-negative bacteria as dependent variables

Dependent variables	Explanatory variables	BE (SE)**	*t*	*p*	Model R^2	*F*	*df*	*p*
#1. IgA claudin-5	Model				0.816	252.29	2/114	< 0.001
	E-cadherin	1.405 (0.063)	22.29	< 0.001				
	CCL-11	0.089 (0.041)	2.16	0.033				
#2. IgA Claudin-5	Model				0.305	24.96	2/114	< 0.001
	IgA Gram− bacteria	0.383 (0.080)	4.81	< 0.001				
	IgA NOX/PRO	0.322 (0.080)	4.04	< 0.001				
#3. IgA Gram− bacteria	Model				0.327	18.30	3/113	< 0.001
	Gut barrier	0.485 (0.079)	6.15	< 0.001				
	Sex	0.341 (0.157)	2.17	0.032				
	Age	0.014 (0.007)	2.14	0.035				
#4. IgA Gram− bacteria	Model				0.333	18.78	3/113	< 0.001
	E-cadherin	0.488 (0.078)	6.26	< 0.001				
	Sex	0.382 (0.155)	2.46	0.016				
	Age	0.015 (0.007)	2.20	0.030				
#5. IgA Gram− bacteria	Model				0.313	17.16	3/113	< 0.001
	Vascular barrier	0.469 (0.079)	5.90	< 0.001				
	Age	0.017 (0.007)	2.60	0.011				
	Sex	0.321 (0.159)	2.02	0.046				

Gut barrier and vascular barrier: see Table 1 for computation

TRYCAT ratio (as toxic substances that possibly could affect the BBB). We found that there was a strong association between IgA claudin-5 and IgA E-cadherin and CCL-11. We found that 30.5% of the variance in IgA to claudin-5 could be explained by the regression on IgA Gram-negative bacteria and IgA NOX/PRO.

We have also examined whether the increased IgA responses to the sum of OD values of five Gram-negative bacteria (dependent variables) in deficit schizophrenia may be predicted by signs of leaky gut and leaky vascular barriers. We found that 32.7% of the variance in IgA Gram-negative bacteria was explained by the gut barrier index or E-cadherin and age and sex (regression #3). Also the vascular index was significantly associated with IgA Gram-negative bacteria (regression #5).

Discussion

The first major finding of this study is that IgA responses to paracellular proteins, E-cadherin, claudin-5, β-catenin, the paracellular index, and the PARA/TRANS ratio were significantly and positively associated with deficit schizophrenia versus nondeficit schizophrenia and controls, while IgA to occludin was significantly associated with deficit schizophrenia versus nondeficit schizophrenia. The distance in the PARA/TRANS ratio between deficit and nondeficit schizophrenia was 1.499 standard deviations, and the distance between deficit schizophrenia and normal controls was 1.569 standard deviations, while the bootstrapped AUC under the ROC curve was 0.93, indicating that the increase in the PARA/TRANS ratio is highly specific for deficit schizophrenia.

The results of the present study extend those of Maes et al. (2019) who found that a comparable ratio based on IgM responses to paracellular and transcellular proteins significantly discriminated deficit patients from controls and patients without deficit syndrome. Nevertheless, the IgA PARA/TRANS ratio computed here is more specific for deficit schizophrenia than the IgM PARA/TRANS ratio (Maes et al. 2019), although both indices are strongly associated ($r = 0.389$, $p < 0.001$, $n = 116$). As such, the *z* unit weighted composite score used in the current study (PARA/TRANS) reflects the combination of increased damage to paracellular TJ and AJ proteins and mild changes in cytoskeletal proteins. In the current study, we found that the IgA responses to EIF (keratin) and talin were significantly lower in patients with deficit schizophrenia, suggesting that this phenotype of schizophrenia may be accompanied by impairments in talin and keratin. Talin is a cytoskeletal protein that binds integrins to the actin cytoskeleton and mediates integrin activation (Klapholz and Brown 2017). Keratin not only gives mechanical support to the cell but also regulates cell growth, survival, and death (Salas et al. 2016). Loss of keratin may induce defective barrier functions including permeabilization of tight junctions and may predispose to inflammation (Salas et al. 2016). Loss of keratin in gut cells may be

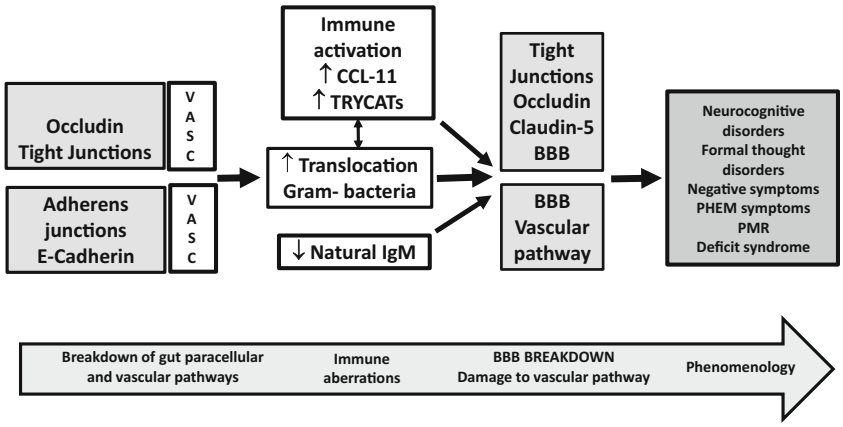

Fig. 3 The association between breakdown of the paracellular tight and adherens junctions and the vascular (VASC) barrier in the gut and the blood brain barrier (BBB) is mediated by bacterial translocation and peripheral immune aberrations, which all together are associated with the phenomenology of schizophrenia. CCL-11 or eotaxin. TRYCATs, tryptophan catabolites; PHEM, psychosis, hostility, excitation, and mannerism; PMR, psychomotor retardation

accompanied by colitis and Th-2 upregulation with T-cell recruitment (Salas et al. 2016). Interestingly, gene expression profiling of the prefrontal cortex of schizophrenia patients showed that the KRT18 gene (encoding type I intermediate filament keratin 18) may be involved in schizophrenia (Mladinov et al. 2016). Previously, it was reported that schizophrenia patients show attenuated adhesion efficiency of fibroblasts, although no significant differences in talin, integrin, and vinculin were found between schizophrenia patients and controls (Miyamae et al. 1998). Nevertheless, it is possible that the mild alterations in cytoskeleton proteins and keratin observed in our studies are secondary to degradation of the TJs and AJs, which in part regulate the cytoskeleton (Balda and Matter 1989; Kuwabara et al. 2001).

As reviewed in the "Introduction," E-cadherin is more specific to the gut barrier and claudin-5 to the BBB, while occludin and β-catenin function in both barriers (van Roy and Berx 2008; Gomez et al. 2015; Brüser and Bogdan 2017; Hartsock and Nelson 2008; Vojdani and Vojdani 2019; Tian et al. 2011; Nelson and Nusse 2004; Rüffer and Gerke 2004). Furthermore, the appearance of IgA antibodies directed against these paracellular proteins in the plasma of patients with deficit schizophrenia suggests a breakdown of the paracellular pathway in the gut and BB barriers (Vojdani and Vojdani 2019). Moreover, since claudin-5 and occludin are key components of the TJs and E-cadherin and β-catenin of the AJs, it is safe to conclude that deficit schizophrenia is characterized by a breakdown of both the TJs and AJs of the paracellular pathways in the gut and BBB. Importantly, in both the gut and BBB, there are cross-talks between TJs and AJs and the cytoskeleton. Firstly, in the BBB, the cross-talk between both TJs and AJs maintains barrier integrity (Tietz and Engelhardt 2015). Secondly, in the gut, aberrations in TJs and AJs may induce dysfunctions in cell–cell adhesion and the actin cytoskeleton (Hartsock and Nelson 2008; Maes et al. 2019), while aberrations in the E-cadherin–β-catenin complex may cause dysfunctions in the Wnt/β-catenin signaling pathway, which plays a key role in cell homeostasis (MacDonald et al. 2009). Therefore, our *z* unit weighted composite scores based on claudin-5, occludin, and β-catenin reflect the reciprocal relationships between these two junctions.

Importantly, new data show that alterations in TJs of the BBB are associated with the progression of many neuroinflammatory disorders, including stroke, Parkinson's and Alzheimer's disease, and multiple sclerosis (Luissint et al. 2012; Webb and Muir 2000). There is also some evidence that schizophrenia may be accompanied by increased BBB permeability (Greene et al. 2018). Recently, it was shown that there is a significant association between a single nucleotide polymorphism in the claudin-5 gene and schizophrenia and that targeted suppression of claudin-5 is accompanied by increased localized BBB permeability (Greene et al. 2018). Moreover, in the BBB, the TJ proteins also integrate and modulate many signaling networks thereby impacting transcriptional control, cytoskeletal rearrangement (Bauer et al. 2014), and the brain endothelial cell phenotype (Stamatovic et al. 2016). Importantly, in the current study, we found significant associations between IgA to claudin-5 and Gram-negative bacteria as well as NOX/PRO TRYCAT ratio and CCL-11. There is evidence that LPS may cause BBB permeabilization and may alter BBB functions, including transport functions and immune cell trafficking (Banks et al. 1999; Xaio et al. 2001; Minami et al. 1998; Ghosh et al. 2014). Furthermore, inflammation may disrupt the TJs thereby promoting paracellular opening of the BBB (Stolp and Dziegielewska 2009; Varatharaj and Galea 2017). Some neurotoxic TRYCATS such as quinolinic acid may also impair BBB integrity (Baranyi et al. 2017), while CCL-11 downregulates TJ proteins (occludin, zona occludens-1, and claudin-1) in a concentration-dependent manner in human coronary artery endothelial cells (Jamaluddin et al. 2009). In addition, CCL-11 is rapidly transported from the blood to the brain with a slow phase of influx preceding a rapid phase, and consequently, CCL-11 accumulates in many brain regions (Erickson et al. 2014). Also, plasma levels of TRYCATS including kynurenine, 3-OH-kynurenine, and quinolinic acid

determine in part the concentrations of quinolinic acid in the brain (Kita et al. 2002). As a consequence, the transport of CCL-11 and TRYCATs through the BBB coupled with upregulated TJ barriers and, thus, increased BBB permeability may cause cumulative effects of those and other (e.g., pro-inflammatory cytokines) neurotoxic and excitotoxic compounds on neuronal cells, for example by producing reactive oxygen species (Sirivichayakul et al. 2018; Maes et al. 2019). Finally, in inflammatory conditions, BBB breakdown may contribute to the ongoing immune-inflammatory response by producing cytokines, chemokines, nitric oxide, and adhesion molecules (Webb and Muir 2000).

The second major finding of this study is that the vascular barrier may be upregulated in deficit schizophrenia as indicated by significantly increased IgA levels directed to β-catenin and PLVAP in deficit versus nondeficit schizophrenia, while the vascular index was significantly higher in deficit than in nondeficit schizophrenia and controls. PLVAP is an important endothelial protein that regulates microvascular permeability and forms the fenestral diaphragms of the caveolae, fenestrae, and trans-endothelial channels (Stan et al. 2004; Bosma et al. 2018). PLVAP has important vascular barrier functions in the gut, as observed in animal models with PLVAP deficiency (Kurolap et al. 2018), and in the BBB where it regulates basal permeability and leukocyte trafficking (Guo et al. 2016). The expression of PLVAP is upregulated in the endothelium of pathological conditions accompanied with increased BBB permeability (e.g., cancer, stroke) (Shue et al. 2008).

The third major finding of this study is that increased bacterial translocation (as assessed with IgA responses to Gram-negative bacteria) is significantly associated with IgA to E-cadherin and the gut barrier index (indicating damage to gut TJs and AJs). These results indicate that the upregulation of the paracellular pathway in deficit schizophrenia has allowed ingress of Gram-negative bacteria leading to breakdown of oral tolerance. Again, these findings are in agreement with our previous study showing that the IgM PARA/TRANS ratio was significantly associated with signs of bacterial translocation (Maes et al. 2019). Moreover, in the present study, we also observed a significant and positive association between IgA levels directed to Gram-negative bacteria and the vascular barrier index. These findings suggest that increased vascular permeability (in the gut) may play a role in increased translocation of Gram-negative bacteria and/or that toxic effects of Gram-negative bacteria have damaged vascular barriers, for example in the BBB.

The fourth major finding is that the IgA PARA/TRANS ratio and increased bacterial translocation coupled with lower IgM to MDA, the immune activation index, and increased CCL-11 explain a large part of the variance in PHEMN symptoms, psychomotor retardation, formal thought disorders, and neurocognitive deficits as well. Phrased differently, cumulative effects of lowered natural IgM, breakdown of the paracellular pathway, increased bacterial translocation, dysfunctions in the vascular pathway, peripheral immune-inflammatory responses, and BBB breakdown determine a large part of the variance in the deficit syndrome in schizophrenia. Natural IgM antibodies have strong immune-regulatory, anti-inflammatory, and antioxidant effects and, in addition, are a key component of the innate, first-line defense against Gram-negative bacteria and other microbiota (Binder 2012; Weismann and Binder 2012; Díaz-Zaragoza et al. 2015). As such, lowered natural IgM to MDA in deficit schizophrenia (Maes et al. 2018b) together with upregulated paracellular and vascular pathways in the gut may be accompanied by a greater impact of Gram-negative gut-commensal bacteria and a greater activation of immune-inflammatory pathways with increased production of noxious TRYCATs and CCL-11. The convergent effects of these various pathways on the vascular pathway and the TJs of the BBB may ultimately lead to breakdown of the BBB, which allows entry of more neurotoxic and excitotoxic compounds in the brain, while BBB breakdown may aggravate the ongoing immune-inflammatory response. The accruing effects of these cascades may cause microglial activation, astrocyte dysfunctions, and ultimately, neuroprogression causing PHEMN symptoms and executive and memory deficits (Sirivichayakul et al. 2018; Maes et al. 2018a, 2019).

One limitation of the current study is that we employed a case–control design which does not allow to establish firm causal associations. Secondly, it would be more informative if we had measured more biomarkers, including the pro-inflammatory cytokines IL-6 and IL-1β, as well as oxidative stress biomarkers.

Figure 3 summarizes our findings. Increased translocation of Gram-negative bacteria in deficit schizophrenia may be caused by upregulation of tight and adherens junctions in the intestinal paracellular pathways and damage to vascular pathways, including PLVAP. The ensuing bacterial or LPS translocation coupled with increased noxious TRYCAT levels and CCL-11 may cause breakdown of the BBB. Cumulative effects of lowered natural IgM, breakdown of the paracellular pathways in gut and BBB, increased bacterial translocation, dysfunctions in the vascular pathways, peripheral immune-inflammatory responses, and BBB breakdown determine a large part of the variance in neurocognitive deficits and the symptoms of schizophrenia and, consequently, the deficit syndrome.

Author's Contributions All the contributing authors have participated in the manuscript. MM and BK designed the study. BK recruited patients and completed diagnostic interviews and rating scale measurements. MM carried out the statistical analyses. All authors (BK, MM, SS, and AV) contributed to the interpretation of the data and writing of the manuscript. All authors approved the final version of the manuscript.

Funding Information The study was supported by the Asahi Glass Foundation, Chulalongkorn University Centenary Academic Development Project and Ratchadapiseksompotch Funds, Faculty of Medicine, Chulalongkorn University, grant numbers RA60/042 (to BK) and RA61/050 (to MM).

Compliance with Ethical Standards

Conflict of Interest The authors declare that they have no conflict of interest.

References

Al-Sadi R, Boivin M, Ma T (2009) Mechanism of cytokine modulation of epithelial tight junction barrier. Front Biosci (Landmark Ed) 14: 2765–2778

Al-Sadi R, Ye D, Boivin M, Guo S, Hashimi M, Ereifej L, Ma TY (2014) Interleukin-6 modulation of intestinal epithelial tight junction permeability is mediated by JNK pathway activation of claudin-2 gene. PLoS One 9(3):e85345

Amara A, Constans J, Chaugier C, Sebban A, Dubourg L, Peuchant E, Pellegrin JL, Leng B, Conri C, Geffard M (1995) Autoantibodies to malondialdehyde-modified epitope in connective tissue diseases and vasculitides. Clin Exp Immunol 101(2):233–238

Andreasen NC (1989) The scale for the assessment of negative symptoms (SANS): conceptual and theoretical foundations. Brit J Psychiatry Suppl 7:49–58

Balda MS, Matter K (1989) Tight junctions. J Cell Sci 111(Pt5):541–547

Balda MS, Matter K (2000) Transmembrane proteins of tight junctions. Semin Cell Dev Biol 11(4):281–289

Banks WA, Kastin AJ, Brennan JM, Vallance KL (1999) Adsorptive endocytosis of HIV-1gp120 by blood-brain barrier is enhanced by lipopolysaccharide. Exp Neurol 156(1):165–171

Baranyi A, Amouzadeh-Ghadikolai O, Lewinski DV, Breitenecker RJ, Stojakovic T, März W, Robier C, Rothenhäusler HB, Mangge H, Meinitzer A (2017) Beta-trace protein as a new non-invasive immunological marker for quinolinic acid-induced impaired blood-brain barrier integrity. Sci Rep 7:43642

Bauer HC, Krizbai IA, Bauer H, Traweger A (2014) "You shall not pass"—tight junctions of the blood brain barrier. Front Neurosci 8: 392

Benjamini Y, Hochberg Y (1995) Controlling the false discovery rate: a practical and powerful approach to multiple testing. J R Stat Soc Ser B Methodol 57:289–300

Binder CJ (2012) Naturally occurring IgM antibodies to oxidation-specific epitopes. Adv Exp Med Biol 750:2–13

Bosma EK, van Noorden CJF, Schlingemann RO, Klaassen I (2018) The role of plasmalemma vesicle-associated protein in pathological breakdown of blood-brain and blood-retinal barriers: potential novel therapeutic target for cerebral edema and diabetic macular edema. Fluids Barriers CNS 15(1):24

Boullerne A, Petry KG, Geffard M (1996) Circulating antibodies directed against conjugated fatty acids in sera of patients with multiple sclerosis. J Neuroimmunol 65(1):75–81

Boullerne AI, Rodriguez JJ, Touil T, Brochet B, Schmidt S, Abrous ND, Le Moal M, Pua JR, Jensen MA, Mayo W, Arnason BG, Petry KG (2002) Anti-S-nitrosocysteine antibodies are a predictive marker for demyelination in experimental autoimmune encephalomyelitis: implications for multiple sclerosis. J Neurosci 22(1):123–132

Bouziat R, Jabri B (2015) Immunology. Breaching the gut-vascular barrier. Science 350(6262):742–743

Bruewer M, Samarin S, Nusrat A (2006) Inflammatory bowel disease and the apical junctional complex. Ann N Y Acad Sci 1072:242–252

Brüser L, Bogdan S (2017) Adherens junctions on the move-membrane trafficking of E-cadherin. Cold Spring Harb Perspect Biol 1:9(3)

Burridge K, Connell L (1983) Talin: a cytoskeletal component concentrated in adhesion plaques and other sites of actin-membrane interaction. Cell Motil 3(5–6):405–417

CANTAB (2018) The most validated cognitive research software. www.cambridgecognition.com/cantab. Accessed 29 April 2019

CERAD (1986) CERAD—an overview: the consortium to establish a registry for Alzheimer's disease. http://cerad.mc.duke.edu/. Accessed 29 April 2019

Cummins PM (2012) Occludin: one protein, many forms. Mol Cell Biol 32(2):242–250

Daverat P, Geffard M, Orgogozo JM (1989) Identification and characterization of anti-conjugated azelaic acid antibodies in multiple sclerosis. J Neuroimmunol 22(2):129–134

Díaz-Zaragoza M, Hernández-Ávila R, Viedma-Rodríguez R, Arenas-Aranda D, Ostoa-Saloma P (2015 Sep) Natural and adaptive IgM antibodies in the recognition of tumor-associated antigens of breast cancer (review). Oncol Rep 34(3):1106–1114

Dohan FC, Grasberger JC (1973) Relapsed schizophrenics: earlier discharge from the hospital after cereal-free, milk-free diet. Am J Psychiatry 130(6):685–688

Dominguez R, Holmes KC (2011) Actin structure and function. Annu Rev Biophys 40:169–186

Duleu S, Mangas A, Sevin F, Veyret B, Bessede A, Geffard M (2010) Circulating antibodies to IDO/THO pathway metabolites in Alzheimer's disease. Int J Alzheimers Dis 2010

Edelblum KL, Turner JR (2009) The tight junction in inflammatory disease: communication breakdown. Curr Opin Pharmacol 9(6):715–720

Elgueta R, Tse D, Deharvengt SJ, Luciano MR, Carriere C, Noelle RJ, Stan RV (2016) Endothelial plasmalemma vesicle-associated protein regulates the homeostasis of splenic immature B cells and B-1 B cells. J Immunol 197(10):3970–3981

Elias BC, Suzuki T, Seth A, Giorgianni F, Kale G, Shen L, Turner JR, Naren A, Desiderio DM, Rao R (2009) Phosphorylation of Tyr-398 and Tyr-402 in occludin prevents its interaction with ZO-1 and destabilizes its assembly at the tight junctions. J Biol Chem 284(3): 1559–1569

Ergün C, Urhan M, Ayer A (2018) A review on the relationship between gluten and schizophrenia: is gluten the cause? Nutr Neurosci 21(7): 455–466

Erickson MA, Morofuji Y, Owen JB, Banks WA (2014) Rapid transport of CCL11 across the blood-brain barrier: regional variation and importance of blood cells. J Pharmacol Exp Ther 349(3):497–507

Faiderbe S, Chagnaud JL, Geffard M (1992) Anti-phosphoinositide autoantibodies in sera of cancer patients: isotypic and immunochemical characterization. Cancer Lett 66(1):35–41

Fasano A (2012a) Zonulin, regulation of tight junctions, and autoimmune diseases. Ann N Y Acad Sci 1258:25–33

Fasano A (2012b) Leaky gut and autoimmune diseases. Clin Rev Allergy Immunol 42(1):71–78

Furuse M, Hirase T, Itoh M, Nagafuchi A, Yonemura S, Tsukita S, Tsukita S (1993) Occludin: a novel integral membrane protein localizing at tight junctions. J Cell Biol 123(6 Pt 2):1777–1788

Geisler F, Leube RE (2016) Epithelial intermediate filaments: guardians against microbial infection? Cells 5(3)

Ghosh A, Birngruber T, Sattler W, Kroath T, Ratzer M, Sinner F, Pieber TR (2014) Assessment of blood-brain barrier function and the neuroinflammatory response in the rat brain by using cerebral open flow microperfusion (cOFM). PLoS One 9(5):e98143

Goldmann WH (2002) Mechanical aspects of cell shape regulation and signaling. Cell Biol Int 26(4):313–317

Gomez GA, McLachlan RW, Wu SK, Caldwell BJ, Moussa E, Verma S, Bastiani M, Priya R, Parton RG, Gaus K, Sap J, Yap AS (2015) An RPTPα/Src family kinase/Rap1 signaling module recruits myosin IIB to support contractile tension at apical E-cadherin junctions. Mol Biol Cell 26(7):1249–1262

Greene C, Kealy J, Humphries MM, Gong Y, Hou J, Hudson N, Cassidy LM, Martiniano R, Shashi V, Hooper SR, Grant GA, Kenna PF, Norris K, Callaghan CK, Islam MD, O'Mara SM, Najda Z,

Campbell SG, Pachter JS, Thomas J, Williams NM, Humphries P, Murphy KC, Campbell M (2018) Dose-dependent expression of claudin-5 is a modifying factor in schizophrenia. Mol Psychiatry 23(11):2156–2166

Guo L, Zhang H, Hou Y, Wei T, Liu J (2016) Plasmalemma vesicle-associated protein: a crucial component of vascular homeostasis. Exp Ther Med 12(3):1639–1644

Hamilton M (1959) The assessment of anxiety states by rating. Br J Med Psychol 32(1):50–55

Hamilton M (1960) A rating scale for depression. J Neurol Neurosurg Psychiatry 23:56–62

Hartsock A, Nelson WJ (2008) Adherens and tight junctions: structure, function and connections to the actin cytoskeleton. Biochim Biophys Acta 1778(3):660–669

Jamaluddin MS, Wang X, Wang H, Rafael C, Yao Q, Chen C (2009) Eotaxin increases monolayer permeability of human coronary artery endothelial cells. Arterioscler Thromb Vasc Biol 29:2146–2152

Kanchanatawan B, Sirivichayakul S, Ruxrungtham K, Carvalho AF, Geffard M, Ormstad H, Anderson G, Maes M (2018a) Deficit, but not nondeficit, schizophrenia is characterized by mucosa-associated activation of the tryptophan catabolite (TRYCAT) pathway with highly specific increases in IgA responses directed to picolinic, xanthurenic, and quinolinic acid. Mol Neurobiol 55(2):1524–1536

Kanchanatawan B, Thika S, Sirivichayakul S, Carvalho AF, Geffard M, Maes M (2018b) In schizophrenia, depression, anxiety, and physiosomatic symptoms are strongly related to psychotic symptoms and excitation, impairments in episodic memory, and increased production of neurotoxic tryptophan catabolites: a multivariate and machine learning study. Neurotox Res 33(3):641–655

Kay SR, Fiszbein A, Opler LA (1987) The positive and negative syndrome scale (PANSS) for schizophrenia. Schizophr Bull 13:261–276

Kirkpatrick B, Buchanan RW, McKenney PD, Alphs LD, Carpenter WT Jr (1989) The schedule for the deficit syndrome: an instrument for research in schizophrenia. Psychiatry Res 30:119–123

Kita T, Morrison PF, Heyes MP, Markey SP (2002) Effects of systemic and central nervous system localized inflammation on the contributions of metabolic precursors to the L-kynurenine and quinolinic acid pools in brain. J Neurochem 82:258–268

Kittirathanapaiboon P, Khamwongpin M (2005) The validity of the Mini International Neuropsychiatric Interview (M.I.N.I.) Thai version. J Ment Health Thai 13(3):125–135

Klapholz B, Brown NH (2017) Talin—the master of integrin adhesions. J Cell Sci 130(15):2435–2446

Kurolap A, Eshach-Adiv O, Gonzaga-Jauregui C, Dolnikov K, Mory A, Paperna T, Hershkovitz T, Overton JD, Kaplan M, Glaser F, Zohar Y, Shuldiner AR, Berger G, Baris HN (2018) Establishing the role of PLVAP in protein-losing enteropathy: a homozygous missense variant leads to an attenuated phenotype. J Med Genet 55(11):779–784

Kuwabara H, Kokai Y, Kojima T, Takakuwa R, Mori M, Sawada N (2001) Occludin regulates actin cytoskeleton in endothelial cells. Cell Struct Funct 26(2):109–116

Luissint AC, Artus C, Glacial F, Ganeshamoorthy K, Couraud PO (2012) Tight junctions at the blood brain barrier: physiological architecture and disease-associated dysregulation. Fluids Barriers CNS 9(1):23

Ma SC, Li Q, Peng JY, Zhouwen JL, Diao JF, Niu JX, Wang X, Guan XD, Jia W, Jiang WG (2017) Claudin-5 regulates blood-brain barrier permeability by modifying brain microvascular endothelial cell proliferation, migration, and adhesion to prevent lung cancer metastasis. CNS Neurosci Ther 23(12):947–960

MacDonald BT, Tamai K, He X (2009) Wnt/beta-catenin signaling: components, mechanisms, and diseases. Dev Cell 17(1):9–26

Maes M, Kanchanatawan B, Sirivichayakul S, Carvalho AF (2018a) In schizophrenia, increased plasma IgM/IgA responses to gut commensal bacteria are associated with negative symptoms, neurocognitive impairments, and the deficit phenotype. Neurotox Res 35:684–698. https://doi.org/10.1007/s12640-018-9987-y

Maes M, Kanchanatawan B, Sirivichayakul S, Carvalho AF (2018b) In schizophrenia, deficits in natural IgM isotype antibodies including those directed to malondialdehyde and azelaic acid strongly predict negative symptoms, neurocognitive impairments, and the deficit syndrome. Mol Neurobiol. https://doi.org/10.1007/s12035-018-1437-6

Maes M, Sirivichayakul S, Kanchanatawan B, Vodjani A (2019) Upregulation of the intestinal paracellular pathway with breakdown of tight and adherens junctions in deficit schizophrenia. Preprints 2019010141. https://doi.org/10.20944/preprints201901.0141.v1

Minami T, Okazaki J, Kawabata A, Kawaki H, Okazaki Y, Tohno Y (1998) Roles of nitric oxide and prostaglandins in the increased permeability of the blood-brain barrier caused by lipopolysaccharide. Environ Toxicol Pharmacol 5(1):35–41

Miyamae Y, Nakamura Y, Kashiwagi Y, Tanaka T, Kudo T, Takeda M (1998) Altered adhesion efficiency and fibronectin content in fibroblasts from schizophrenic patients. Psychiatry Clin Neurosci 52(3):345–352

Mladinov M, Sedmak G, Fuller HR, Babić Leko M, Mayer D, Kirincich J, Štajduhar A, Borovečki F, Hof PR, Šimić G (2016) Gene expression profiling of the dorsolateral and medial orbitofrontal cortex in schizophrenia. Transl Neurosci 7(1):139–150

Nelson WJ, Nusse R (2004) Convergence of Wnt, beta-catenin, and cadherin pathways. Science 303(5663):1483–1487

Nguyen TT, Kosciolek T, Maldonado Y, Daly RE, Martin AS, McDonald D, Knight R, Jeste DV (2018) Differences in gut microbiome composition between persons with chronic schizophrenia and healthy comparison subjects. Schizophr Res S0920-9964(18):30572–20573

Overall JE, Gorham DR (1962) The brief psychiatric rating scale. Psychol Rep 10:799–812

Roomruangwong C, Kanchanatawan B, Sirivichayakul S, Anderson G, Carvalho AF, Duleu S, Geffard M, Maes M (2017) IgA/IgM responses to tryptophan and tryptophan catabolites (TRYCATs) are differently associated with prenatal depression, physio-somatic symptoms at the end of term and premenstrual syndrome. Mol Neurobiol 54(4):3038–3049

Roomruangwong C, Kanchanatawan B, Carvalho AF, Sirivichayakul S, Duleu S, Geffard M, Maes M (2018a) Body image dissatisfaction in pregnant and non-pregnant females is strongly predicted by immune activation and mucosa-derived activation of the tryptophan catabolite (TRYCAT) pathway. World J Biol Psychiatry 19:200–209

Roomruangwong C, Noto C, Kanchanatawan B, Anderson G, Kubera M, Carvalho AF, Maes M (2018b) The role of aberrations in the immune-inflammatory response system (IRS) and the compensatory immune-regulatory reflex system (CIRS) in different phenotypes of schizophrenia: the IRS-CIRS theory of schizophrenia. Preprint, September 2018. https://doi.org/10.20944/preprints201809.0289.v1

Rowland LM, Demyanovich HK, Wijtenburg SA, Eaton WW, Rodriguez K, Gaston F, Cihakova D, Talor MV, Liu F, McMahon RR, Hong LE, Kelly DL (2017) Antigliadin antibodies (AGA IgG) are related to neurochemistry in schizophrenia. Front Psychiatry 8:104

Rüffer C, Gerke V (2004) The C-terminal cytoplasmic tail of claudins 1 and 5 but not its PDZ-binding motif is required for apical localization at epithelial and endothelial tight junctions. Eur J Cell Biol 83(4):135–144

Salas PJ, Forteza R, Mashukova A (2016) Multiple roles for keratin intermediate filaments in the regulation of epithelial barrier function and apico-basal polarity. Tissue Barriers 4(3):e1178368

Shue EH, Carson-Walter EB, Liu Y, Winans BN, Ali ZS, Chen J, Walter KA (2008) Plasmalemmal vesicle associated protein-1 (PV-1) is a marker of blood-brain barrier disruption in rodent models. BMC Neurosci 9:29

Sirivichayakul S, Kanchanatawan B, Thika S, Carvalho AF, Maes M (2018) A new schizophrenia model: immune activation is associated with induction of different neurotoxic products which together determine memory impairments and schizophrenia symptom dimensions. CNS Neurol Disord Drug Targets. https://doi.org/10.2174/1871527317666181119115532

Sirivichayakul S, Kanchanatawan B, Thika S, Carvalho AF, Maes M (2019) Eotaxin, an endogenous cognitive deteriorating chemokine (ECDC), is a major contributor to cognitive decline in normal people and to executive, memory, and sustained attention deficits, formal thought disorders, and psychopathology in schizophrenia patients. Neurotox Res 35(1):122–138

Spadoni I, Pietrelli A, Pesole G, Rescigno M (2016) Gene expression profile of endothelial cells during perturbation of the gut vascular barrier. Gut Microbes 7(6):540–548

Stamatovic SM, Johnson AM, Keep RF, Andjelkovic AV (2016) Junctional proteins of the blood-brain barrier: new insights into function and dysfunction. Tissue Barriers 4(1):e1154641

Stan RV, Tkachenko E, Niesman IR (2004) PV1 is a key structural component for the formation of the stomatal and fenestral diaphragms. Mol Biol Cell 15(8):3615–3630

Stolp HB, Dziegielewska KM (2009) Review: Role of developmental inflammation and blood-brain barrier dysfunction in neurodevelopmental and neurodegenerative diseases. Neuropathol Appl Neurobiol 35(2):132–146

Suzuki T, Elias BC, Seth A, Shen L, Turner JR, Giorgianni F, Desiderio D, Guntaka R, Rao R (2009) PKC eta regulates occludin phosphorylation and epithelial tight junction integrity. Proc Natl Acad Sci U S A 106(1):61–66

Tian X, Liu Z, Niu B, Zhang J, Tan TK, Lee SR, Zhao Y, Harris DC, Zheng G (2011) E-cadherin/β-catenin complex and the epithelial barrier. J Biomed Biotechnol 2011:567305

Tietz S, Engelhardt B (2015) Brain barriers: crosstalk between complex tight junctions and adherens junctions. J Cell Biol 209(4):493–506

Utech M, Mennigen R, Bruewer M (2010) Endocytosis and recycling of tight junction proteins in inflammation. J Biomed Biotechnol 2010:484987

Van den Bossche J, Malissen B, Mantovani A, De Baetselier P, Van Ginderachter JA (2012) Regulation and function of the E-cadherin/catenin complex in cells of the monocyte-macrophage lineage and DCs. Blood 119(7):1623–1633

van Roy F, Berx G (2008) The cell-cell adhesion molecule E-cadherin. Cell Mol Life Sci 65(23):3756–3788

Varatharaj A, Galea I (2017) The blood-brain barrier in systemic inflammation. Brain Behav Immun 60:1–12

Vojdani A, Vojdani E (2019) Food-associated autoimmunities: when food turns your immune system against you. in press

Webb AA, Muir GD (2000) The blood-brain barrier and its role in inflammation. J Vet Intern Med 14(4):399–411

Weismann D, Binder CJ (2012) The innate immune response to products of phospholipid peroxidation. Biochim Biophys Acta 1818(10):2465–2475

Xaio H, Banks WA, Niehoff ML, Morley JE (2001) Effect of LPS on the permeability of the blood-brain barrier to insulin. Brain Res 896(1–2):36–42

Yu AS, McCarthy KM, Francis SA, McCormack JM, Lai J, Rogers RA, Lynch RD, Schneeberger EE (2005) Knockdown of occludin expression leads to diverse phenotypic alterations in epithelial cells. Am J Physiol Cell Physiol 288(6):C1231–C1241

Zachrisson O, Regland B, Jahreskog M, Kron M, Gottfries CG (2002) A rating scale for fibromyalgia and chronic fatigue syndrome (the FibroFatigue scale). J Psychosom Res 52(6):501–509

Publisher's Note Springer Nature remains neutral with regard to jurisdictional claims in published maps and institutional affiliations.